



OPEN Smart flying in challenging skies: How Red Kites adjust wind turbine micro- and meso-avoidance across weather and experience

Moritz Mercker^{1,2}✉, Jan Škrábal^{3,4}, Jan Blew⁵, Thilo Liesenjohann⁵, Maximilian Raab³, Peter Spakovszky³, Martin Kolbe⁶, Stef van Rijn⁷, Thomas Pfeiffer⁸, Christopher Lünig⁹, Rainer Raab³ & Rainhard Raab³

Understanding bird avoidance behaviour at wind turbines is essential for accurate collision risk assessment. We provide one of the first empirical analyses of both micro-avoidance (avoidance of rotor-swept airspace) and meso-avoidance (avoidance of the entire turbine) in Red Kites (*Milvus milvus*), based on high-resolution GPS telemetry integrated with turbine operational data and simulation-based error correction. Red Kites showed consistently high avoidance rates: meso-avoidance averaged ~90% and micro-avoidance ~80%, resulting in an overall avoidance probability of ~98%. Avoidance varied with individual experience—birds with greater prior exposure to turbines showed lower meso-avoidance. Whether this reflects habituation and increased collision risk or improved spatial awareness remains to be investigated. Environmental conditions also modulated avoidance: higher wind speeds and increased cloud cover were associated with stronger avoidance responses. This suggests that under unfavourable weather, Red Kites adopt more cautious flight behaviour that may be associated with lower collision risk. In contrast, turbine-specific features (e.g. tower height or rotor diameter) had no significant effect. These findings indicate that Red Kites flexibly adjust their spatial behaviour in response to turbine exposure and environmental context. By refining species-specific avoidance estimates and identifying mechanisms influencing risk, our findings improve the empirical basis for collision risk assessment in Red Kites and highlight that avoidance behaviour may vary with environmental conditions and turbine experience.

Keywords Avoidance behaviour, Collision risk, *Milvus milvus*, Telemetry, Wind energy, Wind turbines

The rapid expansion of wind energy plays a vital role in global strategies to mitigate climate change^{1,2}. However, this shift toward renewable energy must be reconciled with the protection of biodiversity, particularly for species vulnerable to turbine-related impacts³. Wind turbines (WT) can impact wildlife both directly, through collisions, and indirectly, through behavioural displacement and habitat loss³. Soaring birds such as raptors are believed to be among the most affected, due to their flight characteristics and overlap with high-wind areas^{4–6}.

Turbine collisions have been documented for a range of raptor species, and comparative analyses indicate that large soaring birds may be particularly vulnerable to such interactions⁷. In some regional contexts, turbine-related mortality has raised concerns about potential demographic effects, particularly for species with low reproductive rates and high adult survival such as the Golden Eagle (*Aquila chrysaetos*)⁸. At the same time, many raptor species exhibit behavioural responses when approaching wind turbines, which can substantially reduce the probability of collision. Collision risk is therefore determined not only by the spatial overlap between birds and turbines but also by avoidance behaviour occurring at different spatial scales. Understanding these behavioural

¹Bionum – Consultants in Biostatistics, 21129 Hamburg, Germany. ²Institute of Mathematics, Heidelberg University, 69120 Heidelberg, Germany. ³TB Raab, 2232 Deutsch-Wagram, Austria. ⁴Department of Biology and Wildlife Diseases, Faculty of Veterinary Hygiene and Ecology, University of Veterinary Sciences Brno, Palackého tř. 1946/1, 61242 Brno, Czech Republic. ⁵BioConsult SH, 25813 Husum, Germany. ⁶Rotmilanzentrum am Heineanum, Am Kloster 1, 38820 Halberstadt, Germany. ⁷Deltamilieu Projecten, Edisonweg 53/D, 4382 NV Vlissingen, The Netherlands. ⁸Weimar, Germany. ⁹LEA LandesEnergieAgentur Hessen GmbH, Mainzer Str. 118, 65189 Wiesbaden, Germany. ✉email: mmercker@bionum.de

mechanisms is thus essential for interpreting observed collision rates and for improving the ecological realism of turbine collision risk assessments.

Suggest that raptors (or birds) can detect and avoid wind turbines⁹ (to date, many studies),^{10–12}, raising the need to understand avoidance behaviour as a key mechanism moderating collision risk. WT avoidance occurs at different spatial scales^{9,13,14}: (1) macro-avoidance refers to large-scale detouring around entire wind farms, (2) meso-avoidance to changes in flight paths near individual turbines, and (3) micro-avoidance to last-moment evasive manoeuvres, avoiding the rotor-swept zone or the rotor blades.

While macro- and meso-avoidance have been increasingly well documented (e.g.,^{5,12,15–17}), micro-avoidance remains poorly understood, though it is directly relevant to our understanding of actual collision risk.

Empirical studies show that many large raptors avoid turbines at macro or meso scales. For example, Busse and Rząd¹⁸ reported that Red Kites (*Milvus milvus*) nesting near turbines in Germany rarely flew through nearby wind farms during the breeding season. Migrating Black Kites (*Milvus migrans*) show clear meso-scale deflection patterns at distances of up to 600–800 m from turbines¹². Similarly, Montagu's Harriers (*Circus pygargus*) exhibit strong meso-avoidance of individual turbines, with an estimated avoidance rate of 93.5% when approaching turbines within the rotor height range based on GPS tracking data¹⁷. However, micro-avoidance has been underrepresented in the literature due to technological and methodological barriers.

Four main challenges have historically limited micro-avoidance research: (1) insufficient spatial and temporal resolution of bird movement data (e.g., from previous GPS tracking devices); (2) lack of detailed, time-specific turbine operation data (e.g., blade speed and orientation) which are usually not available in open data bases, (3) the fundamental problem of spatial error in bird movement data, confounding particularly avoidance analyses on small spatial scales, and (4) the difficulty of analysing “last-second-avoidance behaviour” to the rotor blades, as operational data is limited to blade speed, type and rotor orientation but cannot provide exact blade positions in 3D space at any given moment.

With advances in tracking and data integration technologies, the first two of these limitations are being overcome in the current study. High-frequency GPS loggers now allow accurate positional data (to the second) with meter-scale accuracy¹⁷. Simultaneously, collaborations with turbine operators increasingly enable access to real-time turbine metadata.

The statistical correction of GPS error remains critical for deriving valid estimates of micro-avoidance. Even small positional inaccuracies can blur the fine-scale movement patterns around turbines, making sharp avoidance behaviour appear less distinct—or even absent—than it truly is. Therefore, this challenge is being addressed with a suitable modelling approach. The challenge to analyse avoidance behaviour to the rotor blades however still remains and has to be taken into account when interpreting the results of the current study, as only the avoidance to the rotor-swept zone was taken into account, while avoidance to the rotor blades themselves would add on top of the determined value for micro-avoidance.

In this study, we present—to our knowledge—one of the first quantified analyses of micro-avoidance behaviour applied to Red Kites, using an integrated approach. We combined high-resolution GPS telemetry of tagged Red Kites with detailed metadata from WT, including rotor orientation and blade speed at the time of each bird's approach. To address GPS uncertainty, we estimated mean positional errors from the recent literature and applied a simulation-based framework to correct for location error, allowing us to distinguish true micro-avoidance from measurement noise. We assessed avoidance behaviour at multiple spatial scales, with a particular focus on micro-scale events (that have rarely been empirically documented) as well as the meso-avoidance. The analysis of the macro-avoidance is neglected, since different empirical and modelling studies suggest that Red Kites regularly occur within wind parks (e.g.,^{6,19,20}) or even directly demonstrate, that there is no distinct systematic large-scale avoidance or attraction of wind farms with respect to this species^{11,14}. It should be noted, however, that isolated cases of macro-avoidance have been reported for this species¹⁸.

We report absolute values for both micro- and meso-avoidance, providing an estimate of overall avoidance. In addition, we systematically examine which factors—such as weather conditions, turbine parameters, and the bird's prior experience with wind turbines—influence avoidance behaviour at different spatial scales. With this, our study contributes to a more accurate understanding of WT-bird interactions and supports more evidence-based collision risk assessment for wind energy developments. Our findings provide a basis for more species-specific collision risk assessment in Red Kites by refining avoidance estimates and highlighting that avoidance behaviour varies with environmental conditions and prior turbine experience.

Results

Our simulation-based error correction (schematically given in Fig. 1a,b) for the estimation of the micro-avoidance yielded that the spatial GPS-error leads approximately to a halving of the measured vs. the true avoidance value (Fig. 1c). Based on this in conjunction with the analysis of the high frequency Red Kite GPS-tracking data, we estimated the bias-corrected average micro-avoidance by 80.2% (95%-confidence interval: [72.7–85.7%]). This value was based on a Tweedie-regression model without the bird-ID as a random intercept which was favoured during Akaike Information Criterion (AIC)-based analysis (delta (AIC) < 0.1 such that the less complex model is used). In practical terms, this result means that about four-fifths of potential collisions were averted by the kites' immediate flight adjustments avoiding the rotor swept zone. When subsequently applying the predictor selection and final regression analysis to unravel factors influencing the strength of micro-avoidance, we found that only weather-related variables were selected (Fig. 2 and Table 1). In particular, the strength of micro-avoidance increases with both, the local wind speed measured by the WT as well as the local cloud cover (in both cases $P < 0.1$). The effect size for both measures was comparable: in both cases, the micro-avoidance increased from approximately 70% to approximately 90% with the predictor range. Artificially augmenting the additional predictor “wind turbine rotation speed” to the final micro-avoidance model demonstrated however, that it is indeed mainly the direct effect of the wind influencing the micro-avoidance, and not an additional secondary

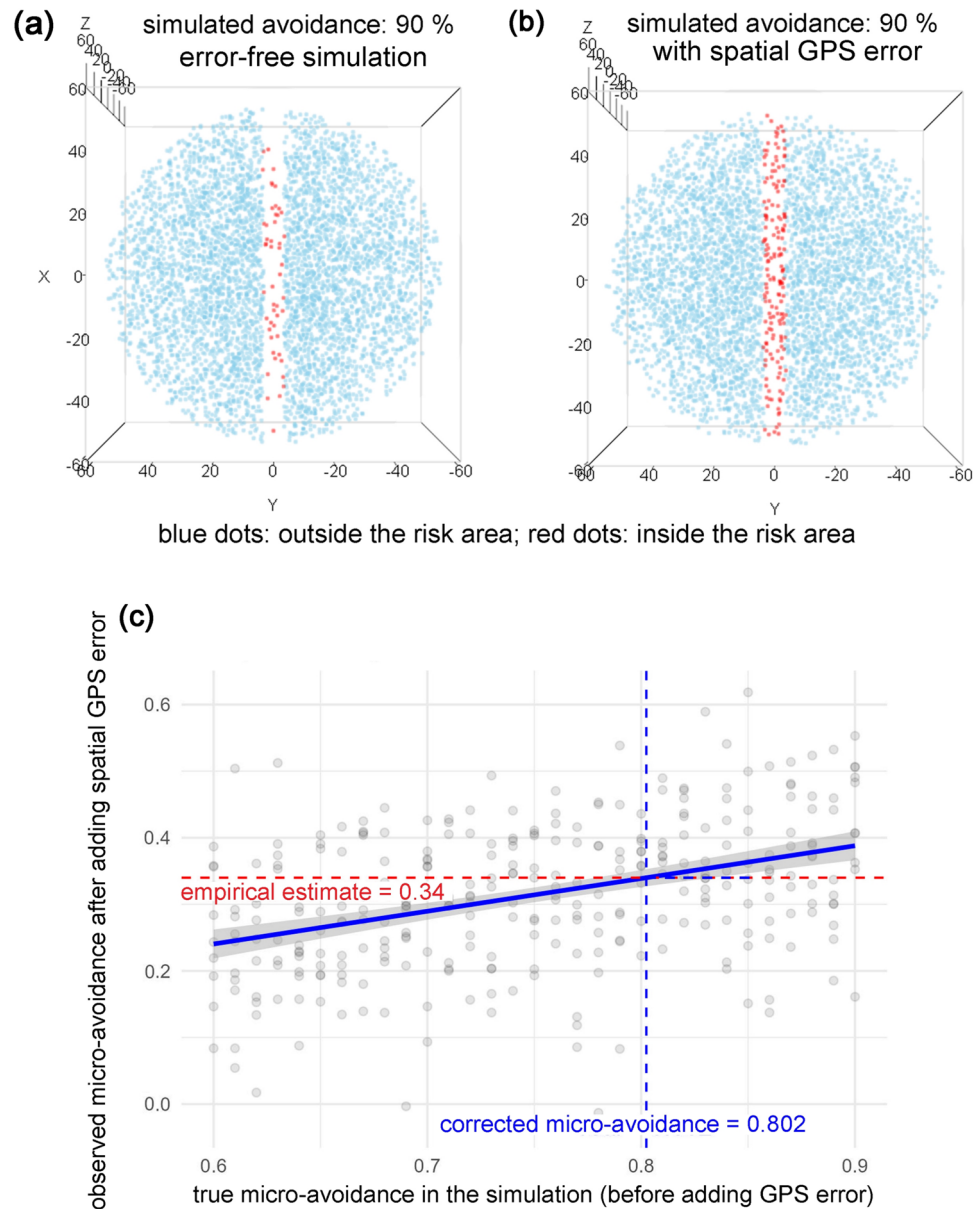


Fig. 1. Illustration of the simulation framework (a–b) and results (c) used to quantify how spatial GPS error biases empirically measured micro-avoidance. (a) Simulated flight positions (blue/red dots) within a three-dimensional wind turbine rotor sphere (side view, such that the cylinder-shaped risk area is viewed perpendicular to its axis). In this example, 90% avoidance of the risk area is simulated without spatial GPS error. Blue dots represent flight positions outside the risk area, red dots positions within it. (b) Same simulation as in (a), but flight positions are stochastically disturbed by an empirically derived average GPS error before classification as “inside” or “outside” the risk area. (c) Relationship between true micro-avoidance in the simulation (x-axis) and the micro-avoidance estimate biased by spatial GPS error (y-axis). The blue solid line shows the Generalised Additive Model (GAM) regression fit, grey-shaded areas indicate 95% confidence intervals, and grey dots represent simulated avoidance values. The empirically measured micro-avoidance based on the real Red Kite GPS data (this study) is indicated by the horizontal red dashed line, and the derived bias-corrected value by the vertical blue dashed line.

effect of the wind turbine rotation speed, since this additional predictor appears to be highly non-significant (Supporting Figure S1).

With respect to the meso-avoidance, we measured an average value of 87.8% [83.9–90.7%] without the bird-ID as a random intercept. However, when introducing this random intercept (as indeed suggested by a distinctly lower AIC-value: $\Delta(\text{AIC}) = 37.3$), the estimate was 5–6% higher with 93.5% [89.4–96.1%]. This difference indicates that birds being frequently in the vicinity of wind turbines (and thus dominating the “simple mean”) show in average a lower meso-avoidance behaviour. Indeed, the results of the finally selected Tweedie-GAMM (cf., Fig. 3 and Table 2) show that beside the low cloud cover (positively correlated with the meso-avoidance),

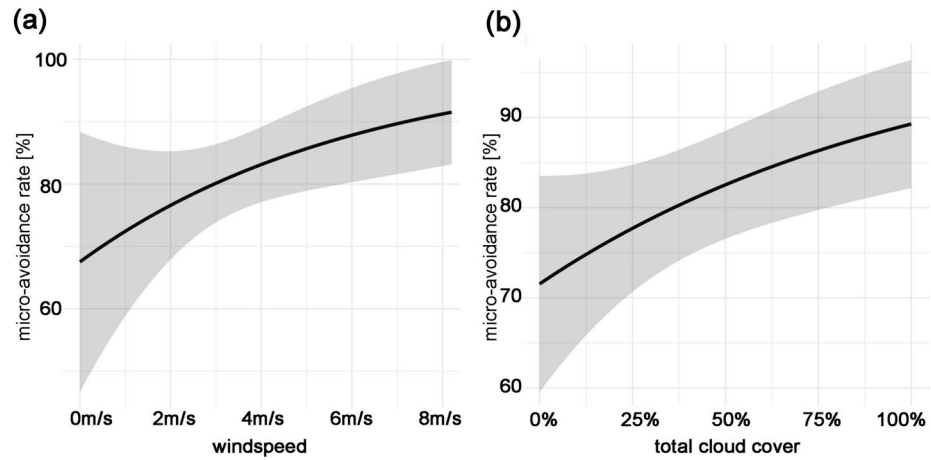


Fig. 2. Micro-avoidance results: Generalized Additive Model (GAM)-based partial effects of Red Kite micro-avoidance rates (y-axes) depending on the predictors finally selected from various weather, wind turbine- and bird wind turbine experience-related variables: **(a)** the wind speed, and **(b)** the total cloud cover. Shaded areas represent 95% confidence bands. Bird identity was not included as a random effect in the model, based on AIC analyses.

AIC	fixed effects
87.9	wind speed, total cloud cover
88.3	wind speed, total cloud cover, low cloud cover
93.9	wind speed, total cloud cover, low cloud cover, experience50, experience500

Table 1. AIC-values and formulas of the three micro-avoidance GAMs with the lowest AIC values. Finally selected model is given in bold letters.

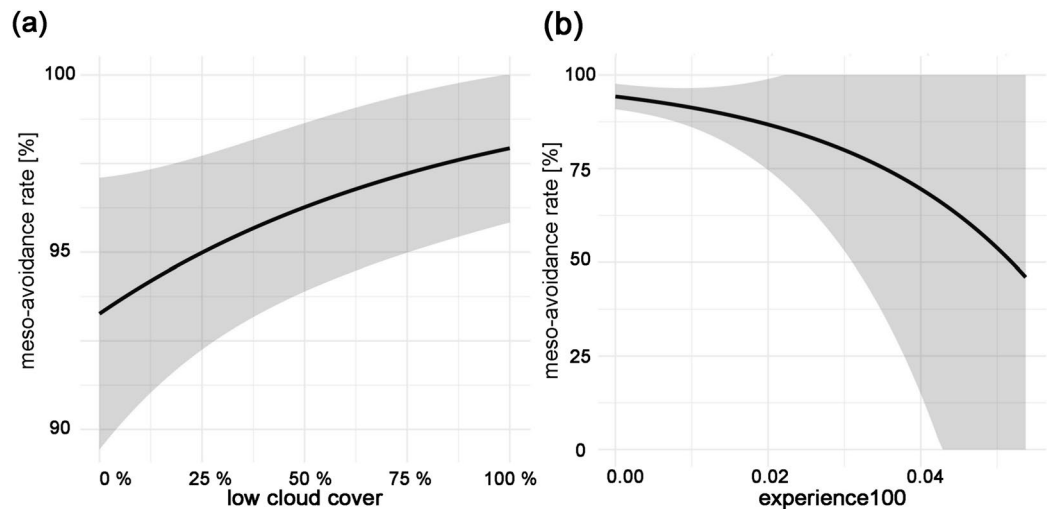


Fig. 3. Meso-avoidance results Generalized Additive Mixed Model (GAMM)-based partial effects of Red Kite meso-avoidance rates (y-axes) depending on the remaining predictors finally selected from various weather, wind turbine- and bird wind turbine experience-related variables: **(a)** the low cloud cover, and **(b)** the experience of each specific birds with respect to wind turbines (up to 100 m distance). Shaded areas represent 95% confidence bands. Bird identity was included as a random effect in the model, based on AIC analyses.

AIC	fixed effects
1662,0	low cloud cover, experience100, wind_speed
1662,5	low cloud cover, experience100
1666,3	low cloud cover

Table 2. AIC-values and formulas of the three meso-avoidance GAMMs with the lowest AIC values. Finally selected model is given in bold letters. Since the first and the second model show a $\Delta(\text{AIC}) < 1.0$, the less complex model is chosen.

also the bird experience with wind turbines is selected. In particular, meso-avoidance decreases distinctly with increasing experience (from nearly 100% to approximately 50%) although the predictor range associated with a lot of experience shows very large confidence intervals. Also here, for both predictors $P < 0.1$.

Thus, in summary we measured meso-avoidance rates of approximately 87–94% and micro-avoidance rates near 80%. If meso- and micro-avoidance are treated as sequential and independent events, the combined probability of avoidance (thus, the total avoidance) equals 1 minus the product of the probabilities of failing each, e.g., $1 - ((1-0.8) \times (1-0.9)) = 98\%$.

Discussion

This study provides rare empirical estimates of turbine micro- and meso-avoidance behaviour in Red Kites, using high-resolution GPS data, turbine operational metadata, and a simulation-based correction for spatial GPS error. Our findings confirm high overall avoidance rates of approximately 98% and reveal previously undocumented variation in avoidance behaviour depending on environmental context and prior individual experience with wind turbines.

Our values of 87–94% micro-avoidance, 80% meso-avoidance and a total avoidance of 98% closely align with prior estimates used in collision risk modelling for Red Kites^{11,14,21}, as well as default assumptions by agencies such as Scottish Natural Heritage^{19,22}. Our results provide empirical confirmation that Red Kites actively and reliably avoid turbines at both meso and micro scales, supporting the continued use of high avoidance values in environmental assessments. These findings reinforce recent findings from Montagu's Harriers¹⁷ and migrating Black Kites¹², but extend them by demonstrating micro-avoidance through telemetry and simulation.

It should be emphasized that the intensity of avoidance behaviour is likely to be highly species-dependent. For example, comparatively limited avoidance behaviour has been suggested for some vulture species due to perceptual constraints related to their visual field configuration. *Gyps* vultures (including *Gyps fulvus* and *Gyps africanus*) possess a relatively small frontal binocular field and large blind areas above, below and behind the head²³. During typical soaring flight, the head is pitched forward so that the visual system provides extensive coverage of the ground below and lateral airspace but may leave a blind area in the direction of travel. As a result, obstacles that intrude into otherwise open airspace, such as wind turbines, may not always be detected in time to allow avoidance²³. More generally, differences in collision vulnerability among bird species have been linked to species-specific traits such as body size, manoeuvrability, flight behaviour and visual perception, which can strongly influence the ability to detect and avoid obstacles²⁴.

We demonstrate that weather variables have a significant influence on avoidance behaviour on both scales. Poor visibility (cloud cover) is associated with increased micro- and meso-avoidance behaviour; the same holds for increased wind, leading to an increase in micro-avoidance. These conditions can worsen visibility (cloudy sky possibly leading to less contrast) and precise navigation (increasing wind/turbulence) during flight, which may lead to more cautious flight behaviour. Here, wind (and thus precise navigation) is particularly important for small-scale movements, aligning with the observation that this variable is selected in the micro-avoidance analysis only. However, we want to point out that our results of the micro-avoidance increasing with the wind concerns moderate winds (up to 8 m/s), since strong winds did not appear in the corresponding data set (N = 69 flights).

These findings suggest that collision risk during inclement weather may not be elevated as previously presumed e.g., for the Golden Eagle⁸. In fact, heightened avoidance under these conditions could even imply a lower risk, in agreement with empirical data on wind turbine bird collisions rarely observing collisions occurring in strong winds²⁵. However, it must be considered here that even a reduction in flight activity and a change in flight altitude with the wind can have a collision-reducing effect, quite independently of changes in active avoidance behaviour.

Our results thus indicate that collision risk may vary with weather conditions because both turbine exposure and avoidance behaviour change with wind speed. In particular, higher wind speeds appear to reduce turbine exposure¹¹ while simultaneously increasing micro-avoidance, potentially providing a “double protection” against collisions. Conversely, moderate-wind, clear-sky conditions may coincide with more frequent flights at rotor height and lower avoidance^{26–28}, highlighting the importance of considering weather-dependent behaviour in collision risk assessments.

An additional key insight of this study is the inverse relationship between experience with turbines and meso-avoidance: individuals with greater prior proximity to turbines exhibited distinctly lower meso-avoidance distances. This fits well with the fact that Red Kites are considered “cultural followers”, which suggests a high degree of species-specific adaptive behaviour (searching for carrion on roads or railway lines, following tractors, etc.)^{29,30}. This pattern is further supported by our finding that the average meso-avoidance value was considerably lower (87.8%) when calculated as a non-weighted average (i.e., dominated by birds with many turbine-near

flights) compared to the estimate derived from the mixed-model approach, where each bird ID contributed equally (93.5%). Similarly, Mercker et al.¹⁴ recently reported a meso-avoidance rate of 86.0% [84.6%–87.3%], primarily based on adult breeding Red Kites during the summer season, when regular contact with turbines within their home ranges is common. Our results extend this understanding by showing that less experienced individuals may exhibit even stronger turbine avoidance.

However, whether reduced avoidance in experienced individuals (driven by age and / or experience with wind turbines) increases or decreases collision risk remains unclear. On one hand, diminished avoidance could reflect reduced caution, elevating the risk. On the other, it may indicate improved spatial awareness and flight control, potentially reducing unnecessary evasion. Complementary findings from Škrábal et al.³¹ support this interpretation. In this recent large-scale mortality analysis based on GPS-tracked Red Kites, collision events were found to vary strongly among wind parks and were primarily associated with turbine characteristics rather than clear differences among age classes. This suggests that although experienced individuals may approach turbines more closely—as indicated by reduced meso-avoidance in our study—their increased familiarity likely enables more precise spatial control, preventing a net increase in collision risk. Thus, experience may simultaneously reduce avoidance distances and maintain effective awareness of turbine structures.

We found no effect of turbine rotor speed (or other turbine-related measures) on avoidance behaviour. This confirms previous experiments with pigeons demonstrating that blade motion does not significantly modulate avoidance of the rotor swept area for this species³². However, a possible way to increase the visibility of turning rotor blades (and the associated “smearing effect”) might be an appropriate painting of the rotor blades to increase the contrast, which was indicated in a lab experiment by Hodos³³ and in a field study considering several bird species (including one raptor, the White-tailed Eagle (*Haliaeetus albicilla*)) by May et al.³⁴. The same principle (high-contrast marking) successfully reduces the risk of collisions with overhead lines³⁵.

It is important to acknowledge a limitation of our micro-avoidance analysis: while we quantify micro-avoidance in terms of evading the rotor-swept volume, our data do not capture instantaneous evasive reactions to blade movement. In other words, our approach measures avoidance at the spatial scale of the rotor-swept area rather than behavioural responses to individual blade movements. True “last-second” micro-avoidance may involve fine motor control and aerial manoeuvres that occur at spatial and temporal scales beyond the resolution of GPS tracking. Consequently, our estimates may not capture all components of micro-avoidance behaviour. In principle, this limitation could bias estimates in either direction: additional last-second avoidance manoeuvres could mean that true avoidance rates are higher than estimated here, whereas turbulent airflow near rotor blades may impair flight control and reduce the ability of birds to evade. Addressing this gap will require observation methods capable of resolving near-blade interactions at very high temporal resolution. High-speed video analysis, including footage from camera-based anti-collision systems (e.g.,³⁶), offers particular promise in this respect, as such systems often record bird–turbine interactions at sub-second resolution. Unfortunately, much of this material currently remains proprietary. Increased data sharing between industry and research could therefore substantially improve our ability to quantify fine-scale avoidance behaviour and refine micro-avoidance estimates. At present, the overall avoidance rate of approximately 98% derived in this study should thus be interpreted as the best available estimate based on telemetry-derived avoidance of the rotor-swept volume, while future studies resolving near-blade behaviour may further refine this value.

Our findings are broadly consistent with avoidance rates around ~98–99% used in collision models for Red Kites but suggest caution against treating avoidance as a strictly static parameter. Behavioural flexibility indicates that avoidance may vary with wind turbine experience and weather conditions. Regulatory assessments could benefit from incorporating a range of avoidance scenarios—e.g., naïve vs. habituated populations—and / or from updating avoidance estimates over the turbine life cycle. Finally, our results reinforce the importance of integrating flight behaviour data (e.g., vertical use of airspace, time of day activity) alongside avoidance rates for a holistic understanding of collision risk^{10,11}.

The present results also have implications for collision risk assessment. Empirical estimates of meso- and micro-avoidance are key parameters in many collision risk models, yet they are often treated as fixed species-specific constants. Our results suggest that avoidance behaviour in Red Kites is high overall but may vary with environmental conditions and turbine experience. Incorporating such context dependence may help improve the ecological realism of future risk assessments. At the same time, the present findings are species-specific and should not be directly transferred to other raptors without further empirical validation. Avoidance behaviour varies substantially among species, and the high avoidance rates reported here for Red Kites should therefore not be interpreted as a general default for other raptor species.

Our results complement recent LIFE EUROKITE analyses focusing on mortality assessment³⁷ and collision determinants³¹. Together, these studies increasingly provide a coherent picture of Red Kite–turbine interactions across Europe. Among nearly 3,000 GPS-tracked birds (of whom only about a third have died so far), only 41 wind turbine collisions were verified³¹, confirming that collisions are comparatively rare and consistent with the high overall avoidance probability of approx. 98% found here. However, the Red Kite is a long-lived species with low reproductive output. Whether this comparatively low proportion, localized collision hotspots or increases in adult mortality may have disproportional demographic effects or not, is still an open question. Bellebaum et al.⁴ reported estimated mortality thresholds of 4.0% due to increasing numbers of wind turbines. They strengthened the need for detailed assessments on the impact on population but assumed a stable population case to be more realistic. This assumption has been confirmed by Gerlach et al.³⁸ postulating a long term stable population trend in Germany. In Austria, Red Kite population is rapidly increasing (BirdLife³⁹), parallel to the increasing number of wind farms. It remains however to be seen how populations will develop under intensive expansion of wind energy. Moreover, mortality causes and collision risks are not evenly distributed across Europe, nor are they equally easy to address politically or technically. As the large-scale expansion of wind energy continues,

No. Individuals (AT/DE)	No. Flights (AT/DE)	No. Turbines (AT/DE)
353 (50/305)	81,310 (1,098/80,212)	846 (20/826)

Table 3. Summary of individuals, flights, and turbines analysed. Values in parentheses indicate data from Austria (AT) and Germany (DE). Two individuals were recorded in both countries.

each country must therefore employ all feasible measures—technological, spatial, and regulatory—to minimise avoidable impacts on vulnerable species.

Materials and methods

Data acquisition and preparation

In this study, GPS telemetry data from 2,943 Red Kites were used as a basis, tagged between 2013 and 2023 as part of the LIFE EUROKITE project (<https://www.life-eurokite.eu>) or contributed by its collaboration partners. From this dataset, we extracted over 5 million GPS locations recorded within a 1 km radius of wind turbines in Austria and Germany for which detailed turbine metadata were available, obtained through direct communication with responsible personnel. We sourced information about the exact location of wind turbines from OpenStreetMap, wind farm operating companies, and the TB Raab database. Each GPS point was spatiotemporally matched with turbine-specific parameters, including rotor inclination, rotational speed, hub height, rotor diameter, as well as wind speed and direction. In cases where rotor inclination was unavailable, a default value of 5° was assigned. Based on this dataset, we identified 81,310 unique flight events, performed by 353 tagged birds (Table 3). A flight was considered valid if it included second-level GPS data with at least two points within the 1 km turbine buffer. If the temporal gap between consecutive points inside the buffer exceeded 60 s, the sequence was considered the start of a new flight. To enrich our dataset with environmental context, we annotated each flight with weather data from the 5th generation atmospheric reanalysis (ERA5) produced by the European Centre for Medium-Range Weather Forecasts (ECMWF), which provides hourly values at a 0.25° spatial resolution. Variables included u and v wind components at 10 m and 100 m height, total and low cloud cover, and precipitation. Finally, to quantify prior exposure to turbines, we calculated an individual-specific experience metric: for each flight, we determined the proportion of GPS points recorded within 50, 100, 200, 250, and 500 m of any wind turbine up to that point in the bird's tracking history. All continuous predictors were visually checked for extreme values by plotting all values and identifying those that were isolated and far from the vast majority of the other values in terms of their value range. In order to avoid distortions of smooth estimates, these obvious outliers/extreme values were conservatively 'capped', i.e. limited to a reasonable maximum value. This upper limit (i.e. the maximum value of predictors shown in the plots) is always to be interpreted below as a 'greater than or equal to' threshold.

Definition of risk area and avoidance metrics

In the context of this study, the “risk area” with respect to the micro-avoidance refers to the portion of airspace within the wind turbine rotor sphere (i.e., a sphere with radius of rotor blade length around the centre of the rotor) in which birds are at acute risk of collision. It encompasses both the space directly swept by the rotor blades and a buffer determined by bird-specific morphology. This buffer accounts for the possibility that even a partial intrusion—such as a wingtip entering the rotor-swept area—can result in a collision. For operationalization, the risk area is approximated as a vertical cylinder with a radius equal to the rotor blade length. The depth of this cylinder comprises the maximum blade chord (adjusted for pitch angle of 15°—cf.¹¹) plus the average body extent of the bird, calculated from body length and wingspan. More details are given in Mercker et al.¹⁴. The risk-areas were calculated separately for each wind turbine where both were considered: the orientation of the WT rotor in the moment the bird was crossing, as well as the horizontal offset of the rotor from the WT tower position.

To quantify avoidance behaviour, we defined scale-specific relative presence metrics based on normalized bird activity within key spatial zones: Micro-avoidance was derived from the proportion of presence within the “risk area”, relative to the presence within the entire “rotor sphere” (rel_{micro}). Meso-avoidance was derived from the relative presence within the rotor sphere compared to the presence within a broader airspace volume surrounding the turbine ($6 * \text{rotor radius}$ —“extended reference volume”) leading to rel_{meso} . Indeed, during meso-avoidance, different birds (including the Red Kite) have been shown to redistribute within this distance^{14,16}. Macro-avoidance (i.e., the avoidance of wind farms on the large scale) was not considered in our study, since several works indicate that there is no corresponding systematic positive or negative bias for the Red Kite on the large scale^{11,14}.

Durations of stay per flight and wind turbine within the above-mentioned spatial zones were corrected for volume and vertical usage by dividing by the durations by the usage-weighted volume of each respective zone (see below). In both cases, lower values of $rel_{micro/meso}$ indicate stronger avoidance, i.e., disproportionately low presence in zones of elevated collision risk. For ease of interpretation, avoidance is expressed as $avoidance = 100 * (1 - rel_{micro/meso})$ [%] so that values closer to 1 represent complete avoidance and values near 0 indicate no avoidance. This transformation was applied in all figures and result summaries, in accordance with standard practice and definitions of avoidance in the literature. For example, a relative use of 20% in a risk area ($rel_{micro} = 0.20$) corresponds to a micro-avoidance rate of 80%. Statistical models were fitted using $rel_{micro/meso}$ as the response variable, since using its reciprocal instead (directly reflecting the attraction of the “reference volume” and thus the avoidance of the smaller risk area) would frequently lead to infinite values,

namely each time the smaller (risk) area was not used during the flight. Where finally estimated avoidance rates always stayed between the meaningful limits [0%, 100%], in some cases, confidence bands partially exceeded these levels and were truncated during visualisation which affects only the graphical representation and does not alter the underlying model estimates.

Correction for spatial error in micro-avoidance estimates

To correct for this spatial uncertainty in the measured positioning of birds relative to wind turbine structures, we applied a simulation-based correction procedure—specifically for micro-avoidance estimates. Since the risk area has a depth of only a few meters, spatial GPS-errors can substantially bias measured micro-avoidance rates, since these errors and the depth of the risk area are within the same order of magnitude. For the estimation of the meso-avoidance, in contrast, we assume that spatial GPS errors are negligible, since here we have a distinct scale separation of errors and the considered dimensions of the considered spatial zones.

To estimate a corresponding correction factor, we simulated three-dimensional point distributions of bird positions within a 3D rotor sphere, using a range of simulated/given avoidance rates (60–90%) based on $N = 310$ simulations of each 1,000 randomly sampled flight positions, leading to a corresponding replacement of these points within the rotor sphere (“avoiding” the risk area). Average rotor radius and average depth of the risk zone were directly extracted from the empirical dataset for parametrisation of this simulation. To mimic spatial GPS measurement error, Gaussian noise was added to the spatial coordinate of each simulated flight point. The standard deviation of these noise distributions was chosen such that the resulting mean 3D positional error (3D Euclidean between true and replaced point) equalled 3.5 m (cf., below for a derivation / plausibilisation of this value). For each simulation sample separately, we subsequently estimated the apparent (biased) micro-avoidance (definitions are given above) after error addition.

Based on the entire data set of simulated values, a Generalised Additive Model^{40,41} with a Gaussian error distribution was then fitted to the relationship between the true avoidance rate (given input parameter in simulations) and the measured avoidance rate (measured output from simulations). The fitted GAM (“correction GAM”) allowed us to finally correct empirically measured micro-avoidance values (i.e., based on real data) for GPS-error-induced bias.

For this final correction of the real data, in a first step, we measured the estimated mean value of the micro-avoidance directly based on the (real world) raw data (using appropriate Tweedie-regression models—cf., below). Given this value and based on the above-derived correction-GAM, we subsequently predicted the corresponding unbiased micro-avoidance value. In a last step, we divided the outcome variable of the (real world) raw data by a correction factor such that the unbiased value was obtained after applying the Tweedie-regression models again.

Importantly, this correction only adjusted the absolute magnitude (y -axis) of the micro-avoidance response variable. It thus did not affect the selection, shape, or relative strength of predictor effects in subsequent regression analyses investigating which factors influence the micro-avoidance. For this reason, the purpose of this correction is to present realistic absolute values of micro-avoidance; however, the main results of this study (i.e., the factors influencing micro-avoidance) remain unaffected by this correction.

Spatial error of high frequency GPS tracks

To account for spatial uncertainty in high frequency GPS data used to track Red Kites, which might affect estimated avoidance rates (cf., above), we assumed a three-dimensional (3D) positional error of 3.5 m in average during our simulation-based approach (cf., above), defined as the expected Euclidean distance between a recorded GPS position and the bird’s true location. This value closely reflects the empirical accuracy of high-frequency GPS loggers (1–3 s intervals) deployed on large raptors and is consistent with performance benchmarks of modern tracking devices under open-sky conditions. Indeed, the following errors have been reported: in average the best expected resolution was 2011 estimated by 5 m⁴², a precision of 3 m was mentioned by Safi et al.⁴³ and spatial errors < 3 m in both, horizontal position and altitude, was recently reported in Schaub et al.¹⁷ based on 3-s tracking data. Taking the values of Schaub et al.¹⁷ as a state-of-the-art estimate for high frequency GPS data, a slightly conservative estimate of 2 m error in each axis (x , y , and z) leads to the 3D Euclidean distance value of $3.464 \approx 3.5$ m which is used in the following.

Correction for vertical airspace use: usage-weighted volumes

To account for the fact that birds do not use vertical airspace uniformly, we corrected all volumetric time measurements using a usage-weighted volume approach. This correction was applied to all three-dimensional spatial zones relevant to avoidance metrics—including the wind turbine rotor sphere, the risk area, and the extended reference volume (sphere of $6 \times$ rotor radius truncated by the ground). Vertical flight activity data were obtained independently from the study by Mercker et al.¹¹, based on a large dataset of high-frequency GPS tracking of Red Kites. From this, a histogram of flight height densities was derived and interpolated into a continuous function. The original values were scaled to produce a proper probability density function, with the integral over the full range equalling 1. For each considered turbine and each above-mentioned spatial zone, we integrated this vertical usage function across the zone’s height bounds (e.g., for the rotor sphere from hub height minus rotor radius to hub height plus rotor radius). This integral, representing the proportion of total vertical use within the height span, was then multiplied by the geometric volume of the zone. The result is a usage-weighted volume with respect to the flight height distribution that reflects not just the size of the airspace, but how often birds occupy it. This is an important issue especially for the large (truncated) sphere (extended reference volume), since it comprises a distinct amount of air space rarely used by this species which would thus bias the avoidance estimates. By dividing observed time values by these usage-weighted volumes, we thus derived normalized presence values for each zone. This allowed unbiased comparison of bird activity across turbines and zones differing in hub height, rotor size, or configuration.

Statistical modelling and predictor selection

To identify environmental and turbine-related factors influencing avoidance behaviour, we used GAMs with a Tweedie distribution, which is well-suited for continuous right-skewed proportional (possibly overdispersed) data with a mass near zero^{44–46}. All models were fitted using the `bam()` function from the `mgcv` package⁴⁷ to allow efficient computation which was required during model selection. Smooth terms were restricted to 3 degrees of freedom ($k=3$) to avoid overfitting and maintain interpretability.

For predictor-selection, we applied a multi-step strategy, combining both model-driven and data-driven approaches:

1. *Shrinkage-based selection in GAMs*: All predictors were initially entered into a full model using `select = TRUE`, which penalizes non-informative terms towards zero.
2. *Regularization via LASSO and Elastic Net*: To identify robust predictors across alternative penalization frameworks, we applied repeated `glmnet()`⁴⁸ fitting (with $\alpha=1$ and 0.5) using both linear and spline-expanded predictors. Predictors were ranked based on their frequency of selection across repeated runs.
3. *Information-theoretic model comparison*: We defined multiple candidate models using and combining predictors selected via GAMs and regularization and compared them using the Akaike Information Criterion (AIC). Final models were selected based on both statistical fit and ecological interpretability.

Notably, we applied slightly different selection thresholds for micro- versus meso-avoidance models. The meso-scale analysis was based on a larger dataset, allowing for the inclusion of a broader set of promising predictors without compromising model stability.

After a first complete run of predictor selection, the final model was (separately for micro- and meso-avoidance) tested via AIC if the bird-ID should be introduced as a random intercept. If this was the case, model selection has been repeated with additionally considering this random intercept (which was possible in the shrinkage-based part of the routine) and in this case the final model was thus given as a Generalised Additive Mixed Model^{49,50} instead of a GAM.

Potential predictor variables

The above-mentioned predictor selection screened a broad set of predictor variables including meteorological parameters (e.g. windspeed, precipitation, cloud cover), turbine-specific attributes (e.g. rotor size, rotation speed, rotor free space), and context-dependent features such as turbine operating status and recent bird experience with wind turbines. Final models retained only a subset of robust predictors, selected based on significance in GAMs/GAMMs, repeated inclusion in regularized regressions (LASSO/Elastic Net), and AIC-based model comparison (cf., above). A complete list of tested predictors and their selection frequencies is provided in Supplementary Table S1.

Data availability

The GPS tracking data used in this study are part of the LIFE EUROKITE project and contain sensitive location information on a protected species. These data cannot be made publicly available due to conservation and data protection restrictions but are available from the corresponding author on reasonable request and with permission from the data holders. Wind turbine operational metadata were provided by turbine operators under confidentiality agreements and cannot be shared publicly. All code used for statistical analyses and simulations is available from the corresponding author upon request.

Received: 17 December 2025; Accepted: 23 March 2026

Published online: 21 April 2026

References

1. Global Wind Energy Council. Global Wind Report 2023. GWEC (2023).
2. International Renewable Energy Agency. World Energy Transitions Outlook: 1.5°C Pathway. IRENA, Abu Dhabi (2021).
3. Marques, A. T. et al. Understanding bird collisions at wind farms: An updated review on the causes and possible mitigation strategies. *Biol. Conserv.* **179**, 40–52. <https://doi.org/10.1016/j.biocon.2014.08.017> (2014).
4. Bellebaum, J., Korner-Nievergelt, F., Dürr, D. & Mammen, U. Wind turbine fatalities approach a level of concern in a raptor population. *J. Nat. Conserv.* **21**, 394–400 (2013).
5. Marques, A. T. et al. Wind turbines cause functional habitat loss for migratory soaring birds. *J. Anim. Ecol.* **89**, 93–103. <https://doi.org/10.1111/1365-2656.12961> (2020).
6. Schaub, M. Spatial distribution of wind turbines is crucial for the survival of red kite populations. *Biol. Conserv.* **155**, 111–118 (2012).
7. Thaxter, C. B. et al. Bird and bat species' global vulnerability to collision mortality at wind farms revealed through a trait-based assessment. *Proc. R. Soc. B Biol. Sci.* **284**, 20170829 (2017).
8. Fielding, A. H. et al. Non-territorial GPS-tagged Golden Eagles *Aquila chrysaetos* at two Scottish wind farms: Avoidance influenced by preferred habitat distribution, wind speed and blade motion status. *PLoS ONE* **16**, 1–26 (2021).
9. Cook, A. S. C. P., Humphreys, E. M., Masden, E. A. & Burton, N. H. K. The Avoidance Rates of Collision Between Birds and Offshore Turbines (Scottish Marine and Freshwater Science No. Volume 5 Number 16). British Trust for Ornithology, The Nunnery, Thetford (GBR) (2014).
10. Linder, A. C., Lyhne, H., Laubek, B., Bruhn, D. & Pertoldi, C. Quantifying raptors' flight behavior to assess collision risk and avoidance behavior to wind turbines. *Symmetry* **14**, 2245. <https://doi.org/10.3390/sym14112245> (2022).
11. Mercker, M., Raab, R., Liesenjohann, T., Liedtke, J. & Blew, J. Fortsetzungsstudie Probabilistik—Das „Raumnutzungs-Kollisionsrisikomodel“ („RKR-Modell“): Fachliche Ausgestaltung einer probabilistischen Berechnungsmethode zur Ermittlung des Kollisionsrisikos von Vögeln an Windenergieanlagen in Genehmigungsverfahren mit Fokus Rotmilan. Im Auftrag des Bundesamtes für Naturschutz, Bonn (2024).

12. Santos, C. D., Ramesh, H., Ferraz, R., Franco, A. M. A. & Wikelski, M. Factors influencing wind turbine avoidance behaviour of a migrating soaring bird. *Sci. Rep.* **12**, 1–8 (2022).
13. May, R. F. A unifying framework for the underlying mechanisms of avian avoidance of wind turbines. *Biol. Conserv.* **190**, 179–187 (2015).
14. Mercker, M., Liedtke, J., Liesenjohann, T. & Blew, J. Pilotstudie „Erprobung Probabilistik“: Erprobung probabilistischer Methoden hinsichtlich ihrer fachlichen Voraussetzungen mit dem Ziel der Validierung der Methode zur Ermittlung des vorhabenbezogenen Tötungsrisikos von kollisionsgefährdeten Brutvogelarten an Windenergieanlagen. Pilotstudie im Auftrag des Hessischen Ministeriums für Umwelt, Klimaschutz, Landwirtschaft und Verbraucherschutz (HMUKLV) (2023).
15. Carlos David, S., Rafael, F., Antonio-Román, M., Alejandro, O. & Martin, W. Black kites of different age and sex show similar avoidance responses to wind turbines during migration. *R. Soc. Open Sci.* <https://doi.org/10.1098/rsos.201933> (2021).
16. Hull, C. L. & Muir, S. C. Behavior and turbine avoidance rates of eagles at two wind farms in Tasmania, Australia. *Wildl. Soc. Bull.* **37**, 49–58 (2013).
17. Schaub, T., Klaassen, R. H. G., Bouten, W., Schlaich, A. E. & Koks, B. J. Collision risk of Montagu's Harriers *Circus pygargus* with wind turbines derived from high-resolution GPS tracking. *Ibis* **162**, 520–534 (2020).
18. Hötker, H., Mammen, K., Mammen, U. & Rasran, L. Red kites and wind farms—telemetry data from the core breeding range. In *Wind Energy and Wildlife Interactions* (ed. Köppel, J.) (Springer, 2017).
19. Urquhart, B. & Whitfield, D. P. Derivation of an avoidance rate for red kite *Milvus milvus* suitable for onshore wind farm collision risk modelling (Natural Research, Banchory, 2016). <https://doi.org/10.13140/RG.2.2.36120.60161>.
20. Busse, P. & Rząd, I. Some data on the behaviour of kites (*Milvus milvus*, *Milvus migrans*) nesting close to two active wind farms in Saxony, Germany. *Ring* **39**, 121–136. <https://doi.org/10.1515/ring-2017-0005> (2017).
21. Reichenbach, M., Greule, S., Steinkamp, T., Reers, H., Akili, J. & Roselius, L. Fachgutachten zur Ermittlung des Flugverhaltens des Rotmilans im Windparkbereich unter Einsatz von Detektionssystemen in Hessen. Publikation in Vorbereitung, Auftraggeber: Hessisches Ministerium für Wirtschaft, Energie, Verkehr und Wohnen; Auftragnehmer: ARSU GmbH (2023).
22. SNH. Avoidance Rates for the onshore SNH Wind Farm Collision Risk Model, October 2016. SNH Guidance Note (2016).
23. Martin, G. R., Portugal, S. J. & Murn, C. P. Visual fields, foraging and collision vulnerability in *Gyps* vultures. *Ibis* **154**, 626–631 (2012).
24. Liesenjohann, M., Blew, J., Fronczek, S., Reichenbach, M. & Bernotat, D. Artspezifische Wirksamkeiten von Vogelschutzmarkern an Freileitungen. Methodische Grundlagen zur Einstufung der Minderungswirkung durch Vogelschutzmarker—ein Fachkonventionsvorschlag (No. BfN-Skripten 537). Bonn—Bad Godesberg (DEU) (2019).
25. Barrios, L. & Rodríguez, A. Behavioural and environmental correlates of soaring-bird mortality at onshore wind turbines. *J. Appl. Ecol.* **41**, 72–81. <https://doi.org/10.1111/j.1365-2664.2004.00876.x> (2004).
26. Aschwanden, J., Stark, H. & Liechti, F. Flight behaviour of Red Kites within their breeding area in relation to local weather variables: Conclusions with regard to wind turbine collision mitigation. *J. Appl. Ecol.* <https://doi.org/10.1111/1365-2664.14739> (2024).
27. Heuck, C. et al. Wind turbines in high quality habitat cause disproportionate increases in collision mortality of the white-tailed eagle. *Biol. Conserv.* **236**, 44–51 (2019).
28. Pfeiffer, T. & Meyburg, B.-U. Flight altitudes and flight activities of adult red kites (*Milvus milvus*) in the breeding area as determined by GPS telemetry. *J. Ornithol.* **163**, 867–879. <https://doi.org/10.1007/s10336-022-01994-1> (2022).
29. Cereghetti, E., Scherler, P., Fattebert, J. & Grüebler, M. U. Quantification of anthropogenic food subsidies to an avian facultative scavenger in urban and rural habitats. *Landsc. Urban Plan.* **190**, 103606. <https://doi.org/10.1016/j.landurbplan.2019.103606> (2019).
30. Orros, M. E. & Fellowes, M. D. E. Widespread supplementary feeding in domestic gardens explains the return of reintroduced Red Kites *Milvus milvus* to an urban area. *Ibis* **157**, 230–238. <https://doi.org/10.1111/ibi.12237> (2015).
31. Škrábal, J. et al. Red kite (*Milvus milvus*) collision risk is higher at wind turbines with larger rotors and lower clearance, evidenced by GPS tracking. *Biol. Conserv.* **312**, 111482. <https://doi.org/10.1016/j.biocon.2025.111482> (2025).
32. Blary, C., Potier, S., Duriez, O., Besnard, A. & Bonadonna, F. Influence of rotation speed and frequency on the decision of *Columba livia domestica* (homing pigeon) to cross the rotor-swept area of paper blades mimicking a wind turbine. *Ornithol. Appl.* **127**, duae058. <https://doi.org/10.1093/ornithapp/duae058> (2025).
33. Hodos, W. Minimization of Motion Smear: Reducing Avian Collisions with Wind Turbines: Period of Performance: July 12, 1999—August 31, 2002. Organization: National Renewable Energy Laboratory (NREL), US Department of Energy (DOE), NREL/SR-500-33249 (2003).
34. May, R. et al. Paint it black: Efficacy of increased wind turbine rotor blade visibility to reduce avian fatalities. *Ecol. Evol.* **10**, 8927–8935. <https://doi.org/10.1002/ece3.6592> (2020).
35. Avian Power Line Interaction Committee, 2012. Reducing Avian Collisions with Power Lines: The state of the art 2012. Edison Electric Institute and APLIC.
36. McClure, C. J. W. et al. Eagle fatalities are reduced by automated curtailment of wind turbines. *J. Appl. Ecol.* **58**, 446–452. <https://doi.org/10.1111/1365-2664.13831> (2021).
37. Panter, C. T. et al. A LEAP forward in wildlife conservation: A standardized framework to determine mortality causes in large GPS-tagged birds. *Ecol. Evol.* **15**, e70975. <https://doi.org/10.1002/ece3.70975> (2025).
38. Gerlach, B. et al. *Vögel in Deutschland - Bestandssituation 2025* (DDA, BfN, LAG VSW, 2025).
39. BirdLife International (Ed.), European Red List of Birds. Publications Office of the European Union, Luxembourg (LUX) (2021).
40. Antoine, G., Thomas C., E. J. & Trevor, H. Generalized linear and generalized additive models in studies of species distributions: setting the scene. *Ecol. Model.* **157**, 89–100 (2002).
41. Hastie, T. & Tibshirani, R. J. *Generalized Additive Models* (Chapman and Hall, 1990).
42. Bridge, E. S. et al. Technology on the move: Recent and forthcoming innovations for tracking migratory birds. *Bioscience* **61**, 689–698. <https://doi.org/10.1525/bio.2011.61.9.7> (2011).
43. Safi, K. et al. Flying with the wind: Scale dependency of speed and direction measurements in modelling wind support in avian flight. *Mov. Ecol.* **1**, 1–13 (2013).
44. Kokonendji, C. C., Demetrio, C. G. B. & Dossou-Gbete, S. Overdispersion and Poisson-Tweedie exponential dispersion models. *Monographie del Seminario Matematico Garcia de Galdeano* **31**, 365–374 (2004).
45. Kokonendji, C. C., Dossou-Gbete, S. & Demetrio, C. G. B. Some discrete exponential dispersion models: Poisson-Tweedie and Hinde-Demetrio classes. *SORT* **28**, 201–214 (2004).
46. Tweedie, M. C. K. An index which distinguishes between some important exponential families. In *Statistics: Applications and New Directions. Proceedings of the Indian Statistical Institute Golden Jubilee International Conference* (eds Gosh, J. K. & Roy, J.) 579–604 (Calcutta (IND), Indian Statistical Institute, 1984).
47. Wood, S. Package 'mgcv'. Package 'mgcv' version 1.7–29. <https://cran.r-project.org/package=mgcv> 1, 729 (2015).
48. Friedman, J., Hastie, T., Tibshirani, R., Narasimhan, B., Tay, K., Simon, N., Qian, J., & Yang, J. glmnet: Lasso and elastic-net regularized generalized linear models. *Astrophysics Source Code Library ascl:2308.011* (2023).
49. Bolker, B. et al. Generalized linear mixed models: A practical guide for ecology and evolution. *Trends Ecol. Evol.* **24**, 127–135. <https://doi.org/10.1016/j.tree.2008.10.008> (2008).
50. Wood, S. *Generalized Additive Models: An Introduction with R*. 2nd ed. (Chapman & Hall/CRC, 2017).

Acknowledgements

We thank Martin Bergmann, Dagmar Adolph, Moritz Röhrs and Brady Mattsson for helpful discussion and proofreading. We also thank the renewable energy companies, namely Alterric, Q Energy, VSB Holding, WLK Energy, WPD, and Enertrag, for providing information on wind turbines. We further thank Matthias Haase and Irene Hoppe for project management in the context of bird tagging. The authors are indebted to all those who assisted in the field with tagging as a part of the LIFE EUOKITE project, without which this study would not be possible.

Author contributions

M.M. conceived the study, developed the methodology, performed the statistical analyses, carried out the simulations, interpreted the results, generated the visualizations, and wrote the original draft of the manuscript. J.Š. led the acquisition, preparation, and processing of GPS and turbine metadata and contributed substantially to data curation. R. Raab (Rainhard) contributed to the conceptual development of the study and to the interpretation of results through extensive scientific discussion. R. Raab (Rainer) established and maintained the long-term data infrastructure enabling the integration of large-scale tracking datasets and contributed to project supervision. M. Raab (Maximilian) assisted in the coordination and consolidation of tracking data streams. R. Raab (Rainer) secured the funding and supported project administration. All authors contributed to biological interpretation, reviewed and edited the manuscript, and approved the final version.

Funding

This work was supported by the European Union via the LIFE EUOKITE project “Cross-border protection of the Red Kite in Europe by reducing human-caused mortality” (LIFE18 NAT/AT/000048). Although co-funded by the European Union, the views and opinions expressed are those of the author(s) only and do not necessarily reflect those of the European Union or CINEA. Neither the European Union nor the granting authority can be held responsible for them.

Declarations

Competing interests

This publication was produced as part of the LIFE EUOKITE project, which is funded by the European Commission's LIFE Nature program (60%), grid operators (15.8%), nature conservation NGOs (9.2%), authorities (8.8%) and renewable energy companies (6.2%). As the LIFE EUOKITE project is based on international cooperation of scientists, NGO, authorities and companies, many people of different background contributed to this study in different ways. Based on the legal setup of the LIFE project, co-financers only provide funding but have no say in the content of scientific contributions. Contributors from private companies and NGOs were largely responsible for tagging birds and providing data to the project, while data evaluation, interpretation and writing of the manuscript was performed by the TB Raab GmbH in cooperation with authors working for independent research institutions. Martin Bergmann, who works for iTerra energy GmbH, conducted a mandated quality assurance review to ensure scientific standards.

Additional information

Supplementary Information The online version contains supplementary material available at <https://doi.org/10.1038/s41598-026-45894-3>.

Correspondence and requests for materials should be addressed to M.M.

Reprints and permissions information is available at www.nature.com/reprints.

Publisher's note Springer Nature remains neutral with regard to jurisdictional claims in published maps and institutional affiliations.

Open Access This article is licensed under a Creative Commons Attribution-NonCommercial-NoDerivatives 4.0 International License, which permits any non-commercial use, sharing, distribution and reproduction in any medium or format, as long as you give appropriate credit to the original author(s) and the source, provide a link to the Creative Commons licence, and indicate if you modified the licensed material. You do not have permission under this licence to share adapted material derived from this article or parts of it. The images or other third party material in this article are included in the article's Creative Commons licence, unless indicated otherwise in a credit line to the material. If material is not included in the article's Creative Commons licence and your intended use is not permitted by statutory regulation or exceeds the permitted use, you will need to obtain permission directly from the copyright holder. To view a copy of this licence, visit <http://creativecommons.org/licenses/by-nc-nd/4.0/>.

© The Author(s) 2026